

Cosmological model-independent test of Λ CDM with two-point diagnostic by the observational Hubble parameter data

Shu-Lei Cao^{1,2}, Xiao-Wei Duan³, Xiao-Lei Meng², Tong-Jie Zhang^{a,1,2}

¹Dezhou University, Dezhou 253023, China

²Department of Astronomy, Beijing Normal University, Beijing, 100875, China

³Department of Astronomy, School of Physics, Peking University, Beijing 100871, China

Received: 08 February 2018 / Accepted: 09 April 2018 / Published online: 19 April 2018

Abstract Aiming at exploring the nature of dark energy (DE), we use forty-three observational Hubble parameter data (OHD) in the redshift range $0 < z \leq 2.36$ to make a cosmological model-independent test of the Λ CDM model with two-point $Om h^2(z_2; z_1)$ diagnostic. In Λ CDM model, with equation of state (EoS) $w = -1$, two-point diagnostic relation $Om h^2 \equiv \Omega_m h^2$ is tenable, where Ω_m is the present matter density parameter, and h is the Hubble parameter divided by 100 km s⁻¹ Mpc⁻¹. We utilize two methods: the weighted mean and median statistics to bin the OHD to increase the signal-to-noise ratio of the measurements. The binning methods turn out to be promising and considered to be robust. By applying the two-point diagnostic to the binned data, we find that although the best-fit values of $Om h^2$ fluctuate as the continuous redshift intervals change, on average, they are continuous with being constant within 1 σ confidence interval. Therefore, we conclude that the Λ CDM model cannot be ruled out.

1 Introduction

Over the past few decades, there have been a number of approaches proposed to quantitatively investigate the expansion history and structure growth of the universe [see 1, 2, for recent reviews]. The observations of Type Ia supernovae (SNIa) [3, 4] have provided ample evidence for an accelerating expansion to an increasing precision [5]. Other complementary probes support that phenomenon, including the baryon acoustic oscillation (BAO) measurements, the weak gravitational lensing, the abundance of galaxy clusters [6], the cosmic microwave background (CMB) anisotropies, the linear

growth of large-scale structure [7], and the Hubble constant H_0 [8]. There are plenty of cosmological models raised to account for the acceleration phenomenon, yet the best-fit one is still uncertain.

The existence of dark energy (DE) with negative equation of state (EoS) parameter $w \equiv p_{DE}/\rho_{DE}$ is considered as a prevailing interpretation currently. In this context, the most popular DE model being used remains to be the simple cosmological constant cold dark matter (Λ CDM) model, with $w = -1$ at all times [9]. However, the popularity of Λ CDM model does not cover the issue that it suffers from fine-tuning and coincidence problems [10, 11]. In addition, it is worth noticing about the possibility of DE with evolving EoS [12], i.e. the dynamical DE models ($w = w(z)$), such as Quintessence [$w > -1$, 13, 14], Phantom [$w < -1$, 15], K-essence [$w > -1$ or $w < -1$, 16, 17], and especially Quintom [w crossing -1, 18, 19] models. Nevertheless, it deserves more profound, physical explanations for all these models. Moreover, Zhao et al. [12] find that an evolving DE can relieve the tensions presented among existing datasets within the Λ CDM framework. Meanwhile, it is useful to introduce diagnostics based upon direct observations and capable of revealing dynamical features of DE. One of these diagnostics is $Om(z)$, which is defined as a function of redshift z [20, 21], i.e.,

$$Om(z) = \frac{\tilde{h}^2(z) - 1}{(1+z)^3 - 1}, \quad (1)$$

with $\tilde{h} = \frac{H(z)}{H_0}$ and $H(z)$ denoting the Hubble expansion rate. $Om(z)$ has the property of being Ω_m for $w = -1$ case. Moreover, Shafieloo et al. [22] modified this diagnostic to accommodate two-point situations as follows,

$$Om(z_2; z_1) = \frac{\tilde{h}^2(z_2) - \tilde{h}^2(z_1)}{(1+z_2)^3 - (1+z_1)^3}. \quad (2)$$

^ae-mail: tjzhang@bnu.edu.cn

In this case, if $Om(z_2; z_1) \equiv \Omega_m$ held for any redshift intervals, it would substantiate the validity of Λ CDM. In other words, the measurements of $Om(z_2; z_1) \neq \Omega_m$ would imply a deviation from Λ CDM and the fact that other DE models with an evolving EoS should be taken into account.

In this paper, we first introduce the measurements of the observational $H(z)$ data (OHD) and then exhibit the currently available data sets in Section 2. In Section 3, we apply two binning methods: the weighted mean and median statistics techniques to OHD, and obtain the binned OHD categorically. In Section 4, based on the binned OHD, we test the Λ CDM model with two-point $Om h^2(z_2; z_1)$ diagnostic. Finally, we summarize our conclusions in Section 5.

2 The observational $H(z)$ data sets

The OHD can be used to constrain cosmological parameters because they are obtained from model-independent direct observations. Until now, three methods have been developed to measure OHD: cosmic chronometers, radial BAO size methods [23], and gravitational waves [24]. Jimenez et al. [25] first proposed that relative galaxy ages can be used to obtain $H(z)$ values and they reported one $H(z)$ measurement at $z \sim 0.1$ in their later work [26]. Simon et al. [27] added additional eight $H(z)$ points in the redshift range between 0.17 and 1.75 from differential ages of passively evolving galaxies, and further constrained the redshift dependence of the DE potential by reconstructing it as a function of redshift. Later, Stern et al. [28] provided two new determinations from red-envelope galaxies and then constrained cosmological parameters including curvature through the joint analysis of CMB data. Furthermore, Moresco et al. [29] obtained eight new measurements of $H(z)$ from the differential spectroscopic evolution of early-type, massive, red elliptical galaxies which can be used as standard cosmic chronometers. By applying the galaxy differential age method to SDSS DR7, Zhang et al. [30] expanded the $H(z)$ data sample by four new points. Taking advantage of near-infrared spectroscopy of high redshift galaxies, Moresco et al. [31] obtained two measurements of $H(z)$. Later, they gained five more latest $H(z)$ values [32]. Recently, Ratsimbazafy et al. [33] provides one more measurement of $H(z)$ based on analysis of high quality spectra of Luminous Red Galaxies (LRGs) obtained with the Southern African Large Telescope (SALT).

On the other side, $H(z)$ can also be extracted from the detection of radial BAO features. Gaztañaga et al. [34] first obtained two $H(z)$ data points using the BAO peak position as a standard ruler in the radial direction.

Blake et al. [35] further combined the measurements of BAO peaks and the Alcock-Paczynski distortion to find three other $H(z)$ results. Samushia et al. [36] provided a $H(z)$ point at $z = 0.57$ from the BOSS DR9 CMASS sample. Xu et al. [37] used the BAO signals from the SDSS DR7 luminous red galaxy sample to derive another observational $H(z)$ measurement. The $H(z)$ value determined based upon BAO features in the Lyman- α forest of SDSS-III quasars were presented by Delubac et al. [38] and Font-Ribera et al. [39], which are the farthest precisely observed $H(z)$ results so far. Alam et al. [40] obtained three $H(z)$ measurements with cosmological analysis of the DR12 galaxy sample.

Moreover, Liu et al. [24] present a new method of measuring Hubble parameter by using the anisotropy of luminosity distance, and the analysis of gravitational wave of neutron star binary system.

After evaluating these data points from [41, 42], we combine these 43 OHD and present them in Table 1 and mark them in Figure 1. Note that it is obvious that the cosmic chronometer method is completely model-independent, and one may misjudge the radial BAO method to be dependent of model since they involve in some fiducial Λ CDM models. However, in fact, the fiducial models cannot affect the results as mentioned in the references (e.g., see P. 5 of Alam et al. [40]). Moreover, the three $H(z)$ measurements taken from Blake et al. [35] are correlated with each other, and also, the three measurements of Alam et al. [40] are correlated. This fact will affect the choice of binning range afterwards.

We use a Λ CDM model with no curvature term to compare theoretical values of Hubble parameter with the OHD results, with the Hubble parameter given by

$$H(z) = H_0 \sqrt{\Omega_m(1+z)^3 + 1 - \Omega_m}, \quad (3)$$

where cosmological parameters take values from the Planck temperature power spectrum measurements [43]. The best fit value of H_0 is $67.81 \text{ km s}^{-1} \text{ Mpc}^{-1}$, and Ω_m is 0.308. The theoretical computation of $H(z)$ based upon this Λ CDM is also shown in Figure 1.

Being independent observational data, $H(z)$ determinations have been frequently used in cosmological research. One of the leading purposes is using them to constrain DE. Jimenez & Loeb [25] first proposed that $H(z)$ measurements can be used to constrain DE EoS at high redshifts. Simon et al. [27] derived constraints on DE potential using $H(z)$ results and supernova data. Samushia & Ratra [44] began applying these measurements to constraining cosmological parameters in various DE models. In the meanwhile, DE evolution came into its own as an active research field in the last twenty years [45–49]. To sum up, the OHD are proved

to be very promising towards understanding the nature of DE.

z	$H(z)$	Method	Ref.
0.0708	69.0 ± 19.68	I	Zhang et al. (2014)-[30]
0.09	69.0 ± 12.0	I	Jimenez et al. (2003)-[26]
0.12	68.6 ± 26.2	I	Zhang et al. (2014)-[30]
0.17	83.0 ± 8.0	I	Simon et al. (2005)-[27]
0.179	75.0 ± 4.0	I	Moresco et al. (2012)-[29]
0.199	75.0 ± 5.0	I	Moresco et al. (2012)-[29]
0.2	72.9 ± 29.6	I	Zhang et al. (2014)-[30]
0.240	79.69 ± 2.65	II	Gaztañaga et al. (2009)-[34]
0.27	77.0 ± 14.0	I	Simon et al. (2005)-[27]
0.28	88.8 ± 36.6	I	Zhang et al. (2014)-[30]
0.35	84.4 ± 7.0	II	Xu et al. (2013)-[37]
0.352	83.0 ± 14.0	I	Moresco et al. (2012)-[29]
0.38	81.5 ± 1.9	II	Alam et al. (2016)-[40]
0.3802	83.0 ± 13.5	I	Moresco et al. (2016)-[32]
0.4	95 ± 17.0	I	Simon et al. (2005)-[27]
0.4004	77.0 ± 10.2	I	Moresco et al. (2016)-[32]
0.4247	87.1 ± 11.2	I	Moresco et al. (2016)-[32]
0.43	86.45 ± 3.68	II	Gaztañaga et al. (2009)-[34]
0.44	82.6 ± 7.8	II	Blake et al. (2012)-[35]
0.4497	92.8 ± 12.9	I	Moresco et al. (2016)-[32]
0.47	89 ± 67	I	Ratsimbazafy et al. (2017)-[33]
0.4783	80.9 ± 9.0	I	Moresco et al. (2016)-[32]
0.48	97.0 ± 62.0	I	Stern et al. (2010)-[28]
0.51	90.4 ± 1.9	II	Alam et al. (2016)-[40]
0.57	92.4 ± 4.5	II	Samushia et al. (2013)-[36]
0.593	104.0 ± 13.0	I	Moresco et al. (2012)-[29]
0.6	87.9 ± 6.1	II	Blake et al. (2012)-[35]
0.61	97.3 ± 2.1	II	Alam et al. (2016)-[40]
0.68	92.0 ± 8.0	I	Moresco et al. (2012)-[29]
0.73	97.3 ± 7.0	II	Blake et al. (2012)-[35]
0.781	105.0 ± 12.0	I	Moresco et al. (2012)-[29]
0.875	125.0 ± 17.0	I	Moresco et al. (2012)-[29]
0.88	90.0 ± 40.0	I	Stern et al. (2010)-[28]
0.9	117.0 ± 23.0	I	Simon et al. (2005)-[27]
1.037	154.0 ± 20.0	I	Moresco et al. (2012)-[29]
1.3	168.0 ± 17.0	I	Simon et al. (2005)-[27]
1.363	160.0 ± 33.6	I	Moresco (2015)-[31]
1.43	177.0 ± 18.0	I	Simon et al. (2005)-[27]
1.53	140.0 ± 14.0	I	Simon et al. (2005)-[27]
1.75	202.0 ± 40.0	I	Simon et al. (2005)-[27]
1.965	186.5 ± 50.4	I	Moresco (2015)-[31]
2.34	222.0 ± 7.0	II	Delubac et al. (2015)-[38]
2.36	226.0 ± 8.0	II	Font-Ribera et al. (2014)-[39]

Table 1: The current available OHD dataset. Where I and II represent the cosmic chronometer and the radial BAO size method, respectively, and $H(z)$ is in units of $\text{km s}^{-1} \text{Mpc}^{-1}$ here.

In the next section, we will bin the OHD in Table 1 by using two binning techniques.

3 Binning OHD

As stated by Farooq et al. [42, 50], there are two techniques: the weighted mean and median statistics, which

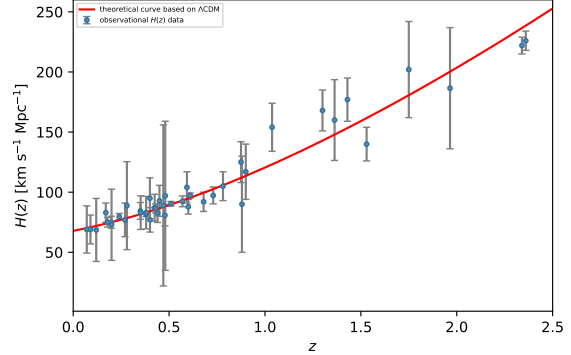


Fig. 1: The full OHD set and theoretical curve of standard flat ΛCDM model. The OHD are represented by gray points along with the uncertainties. The red curve shows theoretical $H(z)$ evolution based upon the adopted ΛCDM model which is described in Section 2.

can be used to bin Hubble parameter measurements. In [42], they listed two reasons to compute “average” $H(z)$ values for bins in redshift space. On the one hand, the weighted mean technique can indicate whether the original data have error bars inconsistent with Gaussianity. On the other hand, the binned data can more clearly visually illustrate tendencies as a function of redshift, without the assumption of a particular cosmological model.

As for the weighted mean technique, the ideal choice should be a trade-off between bin size and number of measurements per bin that maximizes both quantities. In order to avoid correlations at one bin, we choose 3-4, 4-5, 5-6, and 5-6-7 measurements per bin, which separates the correlated data, and the last four measurements are binned by twos for all the cases.

According to Podariu et al. [51], the weighted mean of $H(z)$ is given by

$$\bar{H}(z) = \frac{\sum_{i=1}^N (H(z_i)/\sigma_i^2)}{\sum_{i=1}^N 1/\sigma_i^2}, \quad (4)$$

where $H(z_i)$ and σ_i stand for the Hubble parameter data and the standard deviation for $i = 1, 2, \dots, N$ measurements in the binning redshift range. Similarly, the corresponding weighted bin redshift \bar{z} and weighted error $\bar{\sigma}$ are as follows,

$$\bar{z} = \frac{\sum_{i=1}^N (z_i/\sigma_i^2)}{\sum_{i=1}^N 1/\sigma_i^2}, \quad (5)$$

and

$$\bar{\sigma} = \sqrt{\frac{1}{\sum_{i=1}^N 1/\sigma_i^2}}. \quad (6)$$

The goodness of fit for each bin, the reduced χ_ν^2 , can be expressed as

$$\chi_\nu^2 = \frac{1}{N-1} \sum_{i=1}^N \frac{(H(z_i) - \bar{H}(z))^2}{\sigma_i^2}, \quad (7)$$

where the expected value and error of χ_ν are unity and $1/\sqrt{2(N-1)}$. Thus the number of standard deviations which χ_ν deviates from unity for each bin is presented as

$$N_\sigma = |\chi_\nu - 1| \sqrt{2(N-1)}. \quad (8)$$

Non-Gaussian measurements, the presence of unaccounted for systematic errors, or correlations between measurements can result in large N_σ . The weighted mean results for the binned $H(z)$ measurements are listed in Table 2, where the N_σ values are considerably small for all bins, just like results of Farooq et al. [42], hence indicating that the 43 OHD are not inconsistent with Gaussianity.

Since the median statistics technique originally proposed by Gott et al.[52] has a prerequisite which assumes that measurements of a given quantity are independent and that there are no systematic effects, and as previously mentioned the correlative measurements of OHD from Blake et al. [35] and Alam et al. [40] may contaminate the results, we decide to remove these data for the sake of purity. While other measurements are all uncorrelated and independent with each other, they are more sustainable for evaluation and free of negative influence on the binning results. Table 3 displays the results from median statistics technique. After assuming that there is no overall systematic error in the reduced OHD as a whole and all the remaining measurements are independent, it is convenient to use the median statistics to combine the OHD. As the number of the measurements increases and approaches to infinity, the median can be presented as a true value, therefore, this technique has the merits of reducing the effect of outliers of a set of measurements on the estimate of a true median value. Nevertheless, although OHD are a bit of short in quantity as opposed to the large amount of measurements needed to reveal the true value, we still employ this technique for comparison purpose. If N measurements M_i (where $i = 1, 2, \dots, N$) are consid-

Table 2: Weighted Mean Results for 43 Redshift Measurements, where the unit of $H(z)$ is $\text{km s}^{-1} \text{Mpc}^{-1}$.

Bin N	z	$H(z)$	$H(z)$ (1 σ Range)	$H(z)$ (2 σ Range)	N_σ	
3 or 4 Measurements per Bin						
1	3	0.0895	68.9	59.4-78.5	49.9-88.0	1.98
2	4	0.1847	76.0	73.1-78.9	70.2-81.8	1.12
3	3	0.2412	79.6	77.0-82.2	74.4-84.8	1.56
4	4	0.3776	81.7	79.9-83.5	78.1-85.3	1.85
5	3	0.4095	83.8	76.9-90.7	70.0-97.6	0.61
6	3	0.4329	86.2	83.0-89.4	79.8-92.6	1.02
7	4	0.5086	90.0	88.1-91.9	86.2-93.8	0.98
8	4	0.6024	95.8	94.0-97.6	92.2-99.4	0.06
9	3	0.7201	96.6	91.8-101.4	87.0-106.2	0.71
10	4	0.9287	129.2	118.3-140.1	107.4-151.0	0.07
11	4	1.4301	158.3	149.4-167.2	140.5-176.1	0.05
12	2	1.8331	196.0	164.7-227.3	133.4-258.6	1.07
13	2	2.3487	223.7	218.4-229.0	213.1-234.3	0.88
4 or 5 Measurements per Bin						
1	5	0.1664	75.7	72.4-79.0	69.1-82.3	1.18
2	5	0.2321	78.6	76.3-80.9	74.0-83.2	1.55
3	4	0.3776	81.7	79.9-83.5	78.1-85.3	1.85
4	5	0.4276	85.4	82.4-88.4	79.4-91.4	1.26
5	5	0.5074	90.1	88.3-91.9	86.5-93.7	1.33
6	5	0.6061	95.6	93.8-97.4	92.0-99.2	0.23
7	5	0.7681	102.8	97.3-108.3	91.8-113.8	0.45
8	5	1.3647	157.5	149.3-165.7	141.1-173.9	0.32
9	2	1.8331	196.0	164.7-227.3	133.4-258.6	1.07
10	2	2.3487	223.7	218.4-229.0	213.1-234.3	0.88
5 or 6 Measurements per Bin						
1	5	0.1664	75.7	72.4-79.0	69.1-82.3	1.18
2	5	0.2321	78.6	76.3-80.9	74.0-83.2	1.55
3	6	0.3785	81.7	80.0-83.5	78.2-85.3	1.75
4	6	0.4276	85.7	82.8-88.6	79.9-91.5	1.89
5	5	0.5263	90.7	89.0-92.4	87.3-94.1	1.13
6	6	0.6312	97.5	95.6-99.4	93.7-101.3	0.51
7	6	1.3128	153.0	145.3-160.7	137.6-168.4	0.28
8	2	1.8331	196.0	164.7-227.3	133.4-258.6	1.07
9	2	2.3487	223.7	218.4-229.0	213.1-234.3	0.88
5, 6 or 7 Measurements per Bin						
1	7	0.1767	75.4	72.6-78.2	69.8-81.0	1.80
2	7	0.3333	81.1	79.6-82.6	78.1-84.1	2.27
3	7	0.4288	85.8	82.9-88.7	80.0-91.6	1.71
4	6	0.5247	90.4	88.8-92.0	87.1-93.7	0.89
5	7	0.6331	97.7	95.8-99.6	93.9-101.5	0.55
6	5	1.3647	157.5	149.3-165.7	141.1-173.9	0.32
7	2	1.8331	196.0	164.7-227.3	133.4-258.6	1.07
8	2	2.3487	223.7	218.4-229.0	213.1-234.3	0.88

ered, the probability of finding the true median between values M_i and M_{i+1} is [52]

$$P_i = \frac{2^{-N} N!}{i!(N-i)!}, \quad (9)$$

where $N!$ represents the factorial of N . After applying this technique to the reduced 37 OHD for binning, we obtain the binned results as listed in Table 3, applying the same binning scheme presented above. The

results seem reasonable, but the precision is less than the weighted mean results, which may be caused by the smaller amount of OHD.

Table 3: Median Statistics Results for 37 reduced Redshift Measurements, where the unit of $H(z)$ is $\text{km s}^{-1} \text{Mpc}^{-1}$.

Bin	N	z	$H(z)$	$H(z)$ (1σ Range)	$H(z)$ (2σ Range)
3 or 4 Measurements per Bin					
1	3	0.09	69.0	49.3-88.7	29.6-108.4
2	4	0.189	75.0	68.5-81.5	62.0-88.0
3	3	0.27	79.7	65.7-93.7	51.7-107.7
4	3	0.352	83.0	69.5-96.5	56-110.0
5	4	0.4125	86.8	76.1-97.5	65.4-108.2
6	4	0.474	90.9	53.5-128.4	16.0-165.8
7	4	0.6365	98.2	88.2-108.2	78.2-118.2
8	4	0.89	121.0	99.5-142.5	78.0-164.0
9	4	1.3965	164.0	146.5-181.5	129.0-199.0
10	4	2.1525	212.0	188.0-236.0	164.0-260.0
4 or 5 Measurements per Bin					
1	5	0.12	69.0	57.0-81.0	45.0-93.0
2	5	0.24	77.0	63.0-91.0	49.0-105.0
3	5	0.3802	83.0	69.5-96.5	56.0-110.0
4	5	0.4497	87.1	75.9-98.3	64.7-109.5
5	5	0.593	97.0	85.0-109.0	73.0-121.0
6	4	0.89	121.0	99.5-142.5	78.0-164.0
7	4	1.3965	164.0	146.5-181.5	129.0-199.0
8	4	2.1525	212.0	188.0-236.0	164.0-260.0
4, 5 or 6 Measurements per Bin					
1	5	0.12	69.0	57.0-81.0	45.0-93.0
2	5	0.24	77.0	63.0-91.0	49.0-105.0
3	5	0.3802	83.0	69.5-96.5	56.0-110.0
4	6	0.4598	88.1	76.0-100.2	63.9-112.3
5	6	0.7305	98.2	85.7-110.7	73.2-123.2
6	6	1.3315	157.0	138.0-176.0	119.0-195.0
7	4	2.1525	212.0	188.0-236.0	164.0-260.0
4, 6 or 7 Measurements per Bin					
1	7	0.17	72.9	60.9-84.9	48.9-96.9
2	6	0.315	83.0	69.3-96.8	55.5-110.5
3	7	0.43	87.1	75.9-98.3	64.7-109.5
4	7	0.68	97.0	84.0-110.0	71.0-123.0
5	6	1.3315	157.0	138.0-176.0	119.0-195.0
6	4	2.1525	212.0	188.0-236.0	164.0-260.0

Even though the OHD obtained from the BAO method are model-independent, one can still be confused by the employed fiducial models. Therefore, to avoid the confusion and also for comparison purpose, we decide to exclude the OHD from the BAO method and only consider the cosmic chronometer case, which also have the merit of being independent with each other. Table 4 and 5 present the results from both binning methods. The results are all reasonable as well, and compared to the full binned OHD, the discrepancies are considerably small, which can be seen as evidence of the validity of the OHD derived from the BAO method. Since the dif-

ferent measurements per bin do not significantly affect the results, we can acknowledge the robustness of the binning methods.

Table 4: Weighted Mean Results for Cosmic Chronometer Measurements, where the unit of $H(z)$ is $\text{km s}^{-1} \text{Mpc}^{-1}$.

Bin	N	z	$H(z)$	$H(z)$ (1σ Range)	$H(z)$ (2σ Range)	N_σ
3 or 4 Measurements per Bin						
1	3	0.0895	68.9	59.4-78.5	49.9-88.0	1.98
2	4	0.1847	76.0	73.1-78.9	70.2-81.8	1.12
3	3	0.3089	80.6	71.0-91.2	61.5-99.7	1.46
4	4	0.4035	83.6	77.5-89.7	71.3-95.9	1.06
5	4	0.4691	85.0	77.7-92.3	70.4-99.6	1.34
6	3	0.6866	97.7	91.7-103.6	85.8-109.5	0.51
7	3	0.8834	118.8	105.9-131.7	93.0-144.6	0.85
8	4	1.2798	166.6	156.6-176.6	146.6-186.6	1.20
9	3	1.58	149.3	136.5-162.1	123.7-174.9	0.33
3, 4 or 5 Measurements per Bin						
1	5	0.1664	75.7	72.4-79.0	69.1-82.3	1.18
2	5	0.2221	76.1	71.7-80.5	67.3-84.9	1.90
3	5	0.412	85.3	79.8-90.8	74.2-96.4	1.17
4	5	0.5897	90.1	84.7-85.5	79.3-100.9	0.70
5	4	0.5074	111.4	102.6-120.2	93.8-129	0.86
8	4	1.2798	166.6	156.6-176.6	146.6-186.6	1.20
9	3	1.58	149.3	136.5-162.1	123.7-174.9	0.33
5 or 6 Measurements per Bin						
1	5	0.1664	75.7	72.4-79.0	69.1-82.3	1.18
2	5	0.2221	76.1	71.7-80.5	67.3-84.9	1.90
3	5	0.412	85.3	79.8-90.8	74.2-96.4	1.17
4	5	0.5897	90.1	84.7-85.5	79.3-100.9	0.70
5	5	0.8622	118.3	110.2-126.4	102.2-134.4	0.36
6	6	0.6312	161.1	152.5-169.7	143.9-178.3	0.16

4 Testing the ΛCDM model with $Om h^2(z_2; z_1)$ diagnostic

In our analysis, the validity of $Om h^2(z_2; z_1)$ diagnostic can be tested using $H(z)$ results from cosmological independent measurements. On the basis of the above section, we apply binned OHD from both the weighted mean technique and the median statistics technique to the two-point $Om h^2(z_2; z_1)$ diagnostic.

If $Om(z_2; z_1)$ is always a constant at any redshifts, then it demonstrates that the DE is of the cosmological constant nature. In order to compare directly with the results from CMB, Sahni et al. [53] introduced a more convenient expression of the two-point diagnostic, i.e.,

$$Om h^2(z_2; z_1) = \frac{h^2(z_2) - h^2(z_1)}{(1+z_2)^3 - (1+z_1)^3}, \quad (10)$$

where $h(z) = H(z)/100 \text{ km s}^{-1} \text{Mpc}^{-1}$. The binned $H(z)$ points calculated based upon the aforementioned

Table 5: Median Statistics Results for Cosmic Chronometer Measurements, where the unit of $H(z)$ is $\text{km s}^{-1} \text{Mpc}^{-1}$.

Bin	N	z	$H(z)$	$H(z)$ (1σ Range)	$H(z)$ (2σ Range)
3 or 4 Measurements per Bin					
1	3	0.09	69.0	49.3-88.7	29.6-108.4
2	4	0.189	75.0	68.5-81.5	62.0-88.0
3	3	0.28	83.0	69.0-97.0	55.0-111.0
4	4	0.4002	85.1	72.7-97.4	60.4-109.8
5	4	0.4741	90.9	53.5-128.4	16.0-165.8
6	3	0.68	104.0	92.0-116.0	80.0-128.0
7	3	0.88	117.0	94.0-140.0	71.0-163.0
8	4	1.3315	164.0	145.0-183.0	126.0-202.0
9	3	1.75	186.5	146.5-226.5	106.5-266.5
3, 4 or 5 Measurements per Bin					
1	5	0.12	69.0	57.0-81.0	45.0-93.0
2	5	0.27	77.0	63.0-91.0	49.0-105.0
3	5	0.4004	87.1	74.2-100.0	61.3-112.9
4	5	0.48	92.0	79.0-105.0	66.0-118.0
5	4	0.8775	111.0	91.0-131.0	71.0-151.0
6	4	1.3315	164.0	145.0-183.0	126.0-202.0
7	3	1.75	172.5	146.5-226.5	106.5-266.5
5 or 6 Measurements per Bin					
1	5	0.12	69.0	57.0-81.0	45.0-93.0
2	5	0.27	77.0	63.0-91.0	49.0-105.0
3	5	0.4004	87.1	74.2-100.0	61.3-112.9
4	5	0.48	92.0	79.0-105.0	66.0-118.0
5	5	0.88	117.0	97.0-137.0	77.0-157.0
6	6	1.48	172.5	146.7-198.3	120.9-224.1

binning methods in each case therefore yield $N(N-1)/2$ model-independent measurements of the $Om h^2(z_2; z_1)$ diagnostic, as shown in Figs. 2-7, where the uncertainty $\sigma_{Om h^2(z_2; z_1)}$ can be expressed as follows,

$$\sigma_{Om h^2(z_2; z_1)}^2 = \frac{4 \left(h^2(z_2) \sigma_{h(z_2)}^2 + h^2(z_1) \sigma_{h(z_1)}^2 \right)}{\left((1+z_2)^3 - (1+z_1)^3 \right)^2}. \quad (11)$$

For Λ CDM, we have $Om h^2 \equiv \Omega_m h^2$. The value of $\Omega_m h^2$ is constrained tightly by the Planck observations to be centered around 0.14 for the base of Λ CDM model fit [43]: the Planck temperature power spectrum data alone gives 0.1426

± 0.0020 , the Planck temperature data with lensing reconstruction gives 0.1415 ± 0.0019 , and the Planck temperature data with lensing and external data gives 0.1413 ± 0.0011 , all at 1σ confidence level (CL). As stated in [43], we conservatively select 0.1415 ± 0.0019 as the Planck value. If the Λ CDM model can hold, we would expect a constant value of $Om h^2$ at any redshift intervals. Sahni et al. [53] compared their results with the Planck value to check the validity of the Λ CDM model. From our perspective, we should not follow their goals to test the tension between our results and the Planck value. Instead, we should first consider whether

the values of $Om h^2$ are constant or not. Here we only use the Planck value for comparison purpose.

As shown in Fig. 2, the results from the weighted mean cases, within 1σ confidence interval, are mostly continuous with both being constant (on average) and the Planck value, although some exceptions are presented and the best-fit $Om h^2(\Delta z)$ values fluctuate. Also, as shown in Fig. 3, the results from the median statistic cases are all continuous with both being constant and the Planck value within 1σ confidence interval. Note that these results are not continuous redshift intervals, it only shows the differences for different Δz . Therefore, it would be useful if we plot the continuous results alone to extrapolate the outcomes. Then we illustrate these results with the binned OHD from both binning methods in Figs. 4, which shows that the values of $Om h^2$ for both binning methods fluctuate as the continuous redshift intervals change. The difference between the results from the weighted mean binning data and results from mean statistics is that the fluctuations from the former situation are more intense which makes the tendency more distinct from the first four panels of Fig. 4. Thus, it is fair to come up with the conclusion that the validity of Λ CDM is preserved.

Also, after binning the OHD from the cosmic chronometer method, the corresponding $Om h^2$ results with both binning techniques are demonstrated in Figs. 5-7. It is evident that the fluctuations of the best-fit $Om h^2$ values are more intense than the results from full binned OHD for both binning methods. However, on average, the results are constant at 1σ region. Hence, due to the two-point $Om h^2(z_2; z_1)$ diagnostic combined with binned OHD results, the Λ CDM model is favored. However, we note that the error bars of these results are much bigger than the Planck result, therefore we can only conclude that the flat Λ CDM model cannot be ruled out.

5 Conclusions and Discussions

In this paper, motivated by the investigations on the nature of DE, we test the validity of Λ CDM with the two-point $Om h^2(z_2; z_1)$ diagnostic by using 43 observational $H(z)$ data (OHD) which are obtained from the cosmic chronometers and BAO methods.

Firstly, instead of direct employment of the OHD on the $Om h^2(z_2; z_1)$ diagnostic, we introduce the two binning methods: the weighted mean and median statistics to reduce the noise in the data. After binning OHD, we conclude that the original OHD are not inconsistent with Gaussianity, and the binned data are all reasonable as Tables 2 and 3 displayed. The OHD derived from the

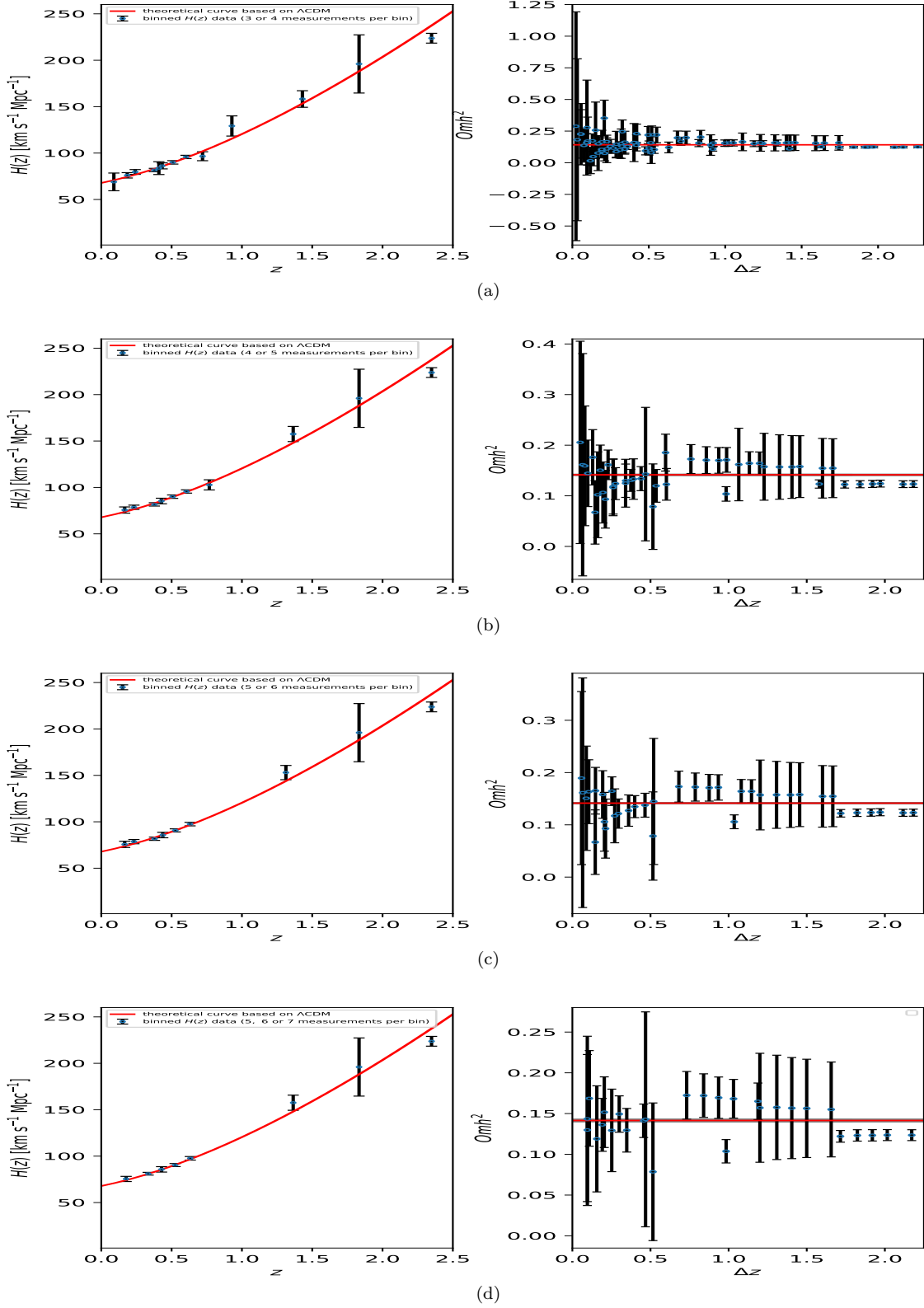


Fig. 2: Binned $H(z)$ data based on full OHD and its corresponding $Om h^2$ diagnostic values for the weighted mean technique. The panels (a), (b) (c) and (d) present the 3-4, 4-5, 5-6 and 5-6-7 measurements per bin case, respectively, where the red lines and grey shaded regions in the right panels represent the best-fit value of $Om h^2$ and its uncertainties retrieved from the Planck CMB data.

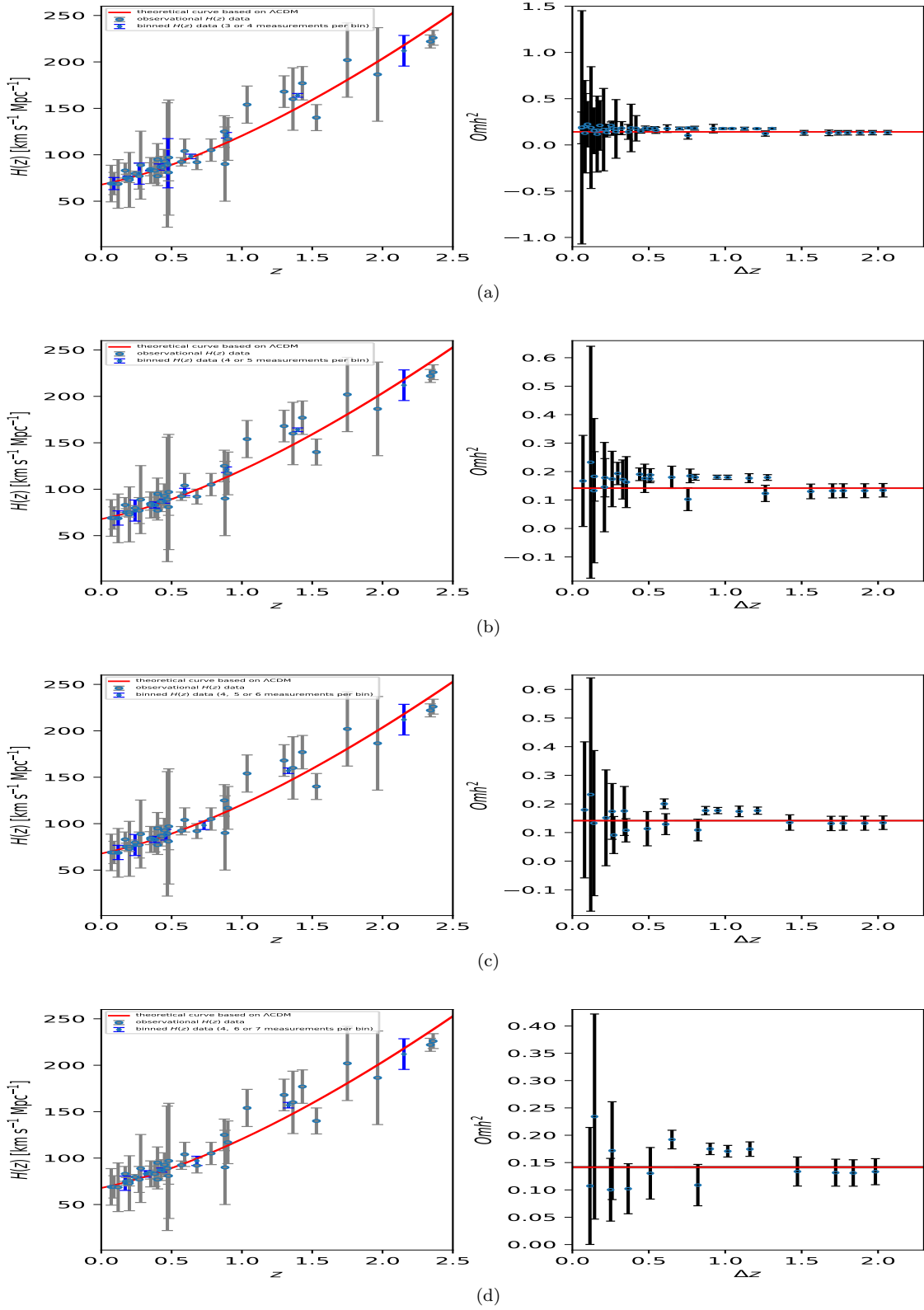


Fig. 3: 37 reduced OHD associated with binned data and its corresponding $Om h^2$ diagnostic values for the median statistics technique. The panels (a), (b) (c) and (d) present the 3-4, 4-5, 4-5-6 and 4-6-7 measurements per bin case, respectively, where the red lines in the right panels represent the best-fit value of $Om h^2$ retrieved from the Planck CMB data.

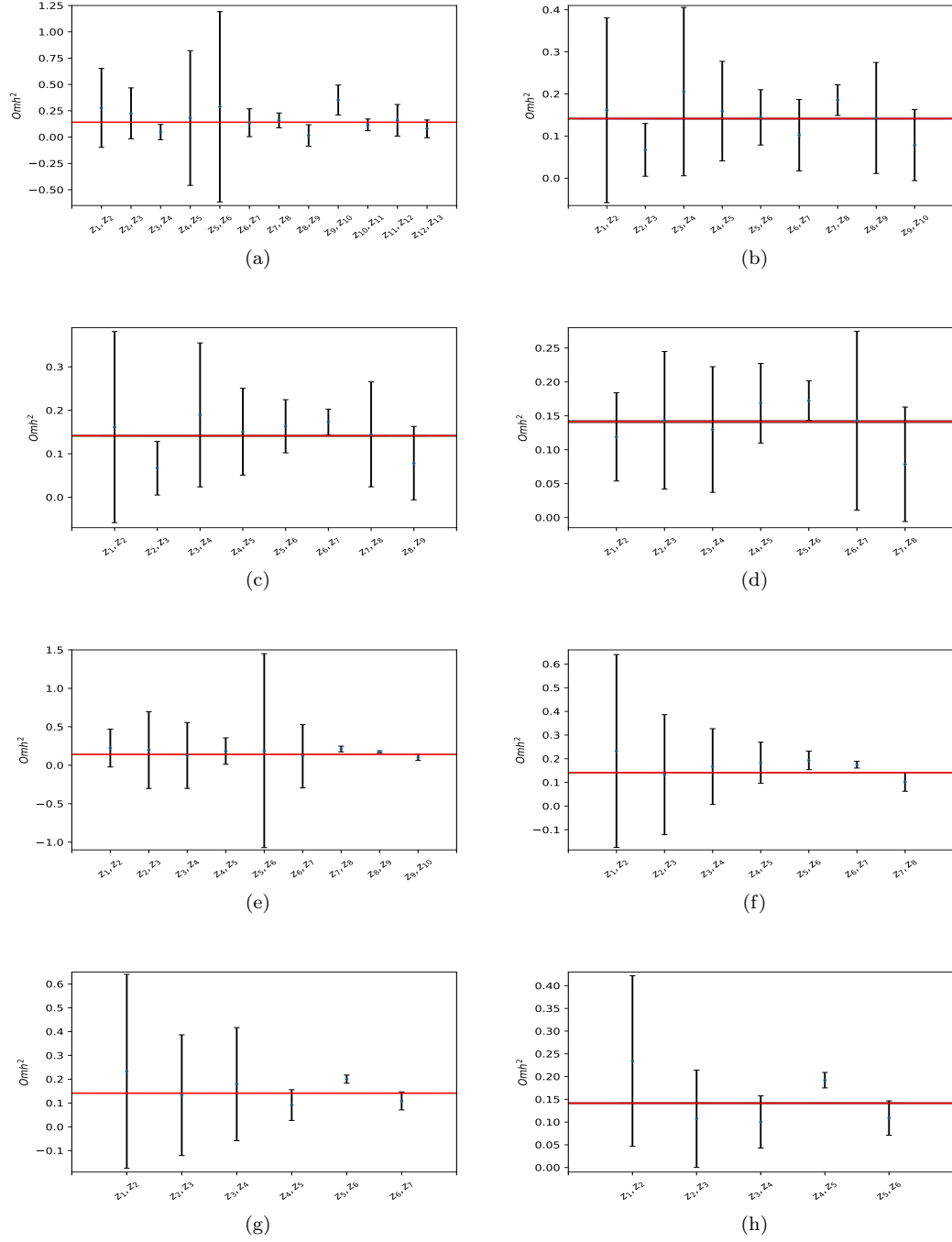


Fig. 4: $Om h^2$ diagnostic values for both the weighted mean and median statistics techniques with respect to continuous redshifts. The panels (a), (b), (c) and (d) present the weighted mean 3-4, 4-5, 5-6, and 5-6-7 measurements per bin, respectively. The panels (e), (f) (g) and (h) present the median statistics 3-4, 4-5, 4-5-6 and 4-6-7 measurements per bin case, respectively, where the red lines represent the best-fit value of $Om h^2$ retrieved from the Planck CMB data.

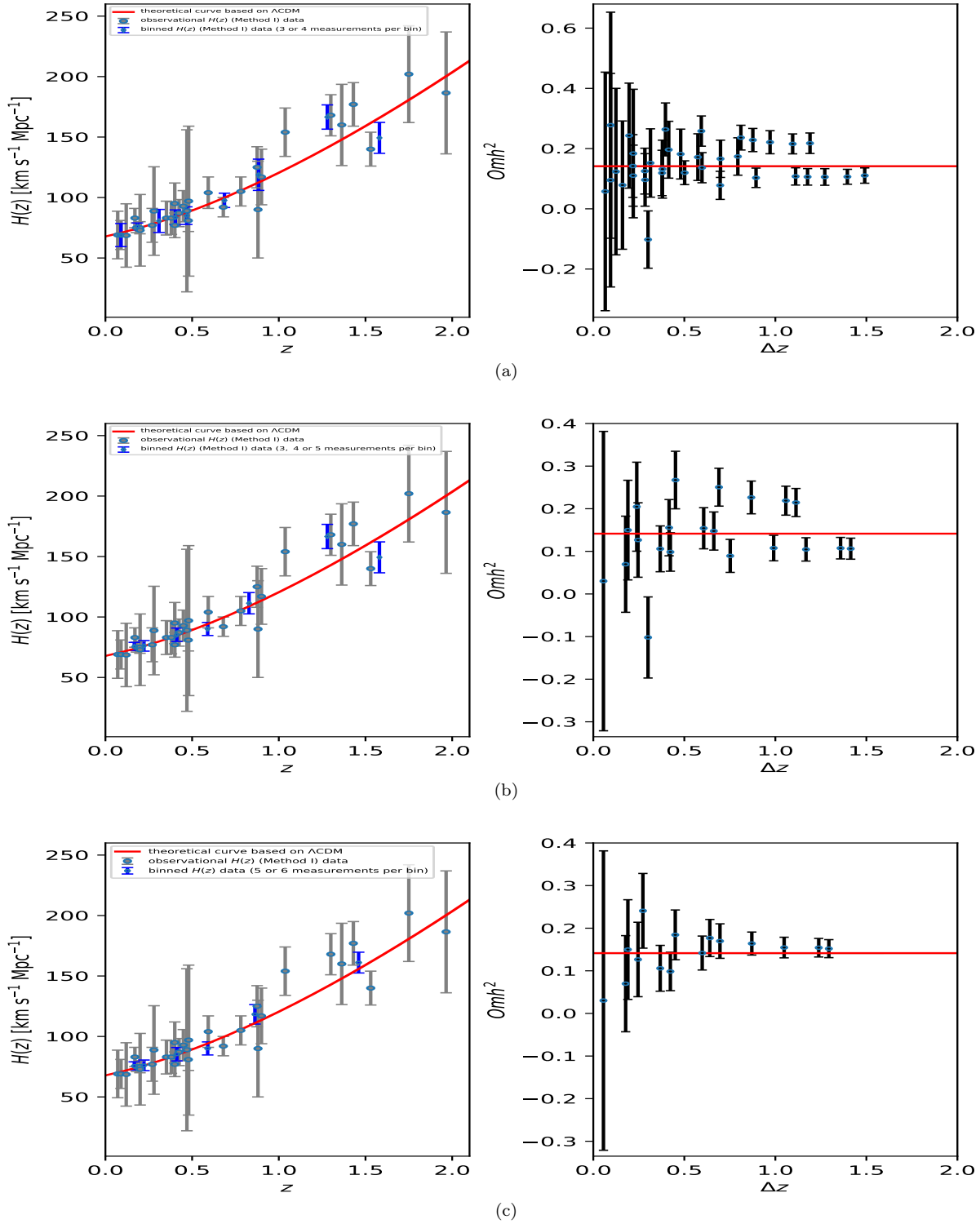
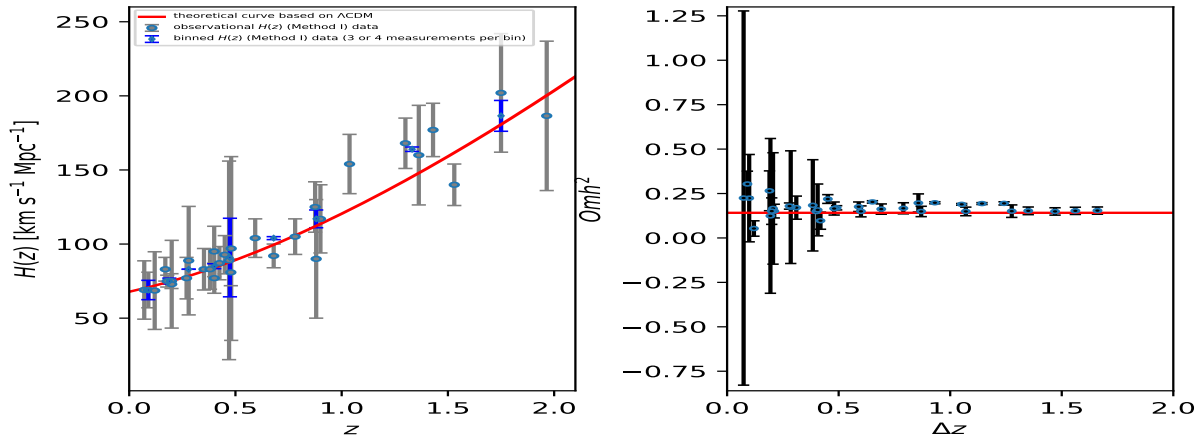
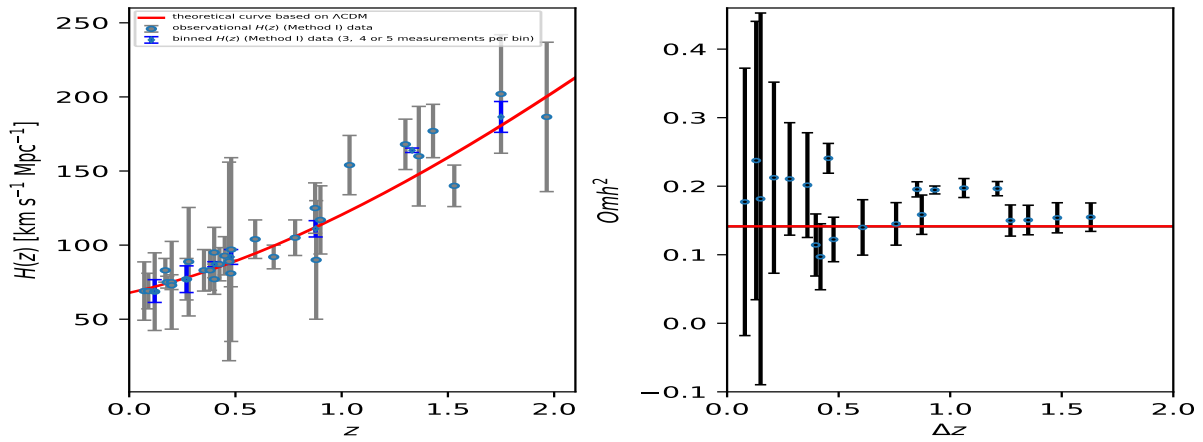


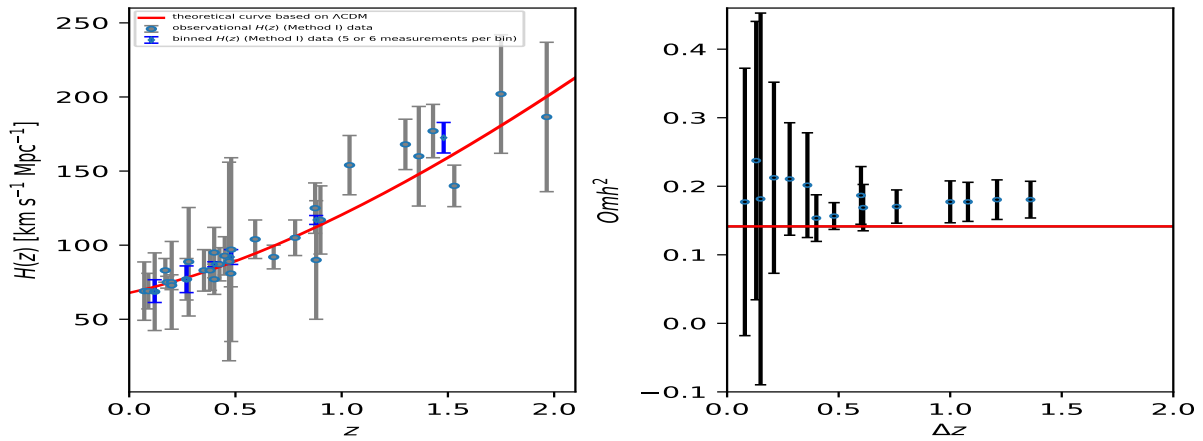
Fig. 5: OHD from the cosmic chronometer method associated with binned data and its corresponding $Om h^2$ diagnostic values for the weighted mean technique. The panels (a), (b) and (c) present the 3-4, 3-4-5 and 5-6 measurements per bin case, respectively, where the red lines in the right panels represent the best-fit value of $Om h^2$ retrieved from the Planck CMB data.



(a)



(b)



(c)

Fig. 6: Same as Fig. 5, but for the median statistics technique.

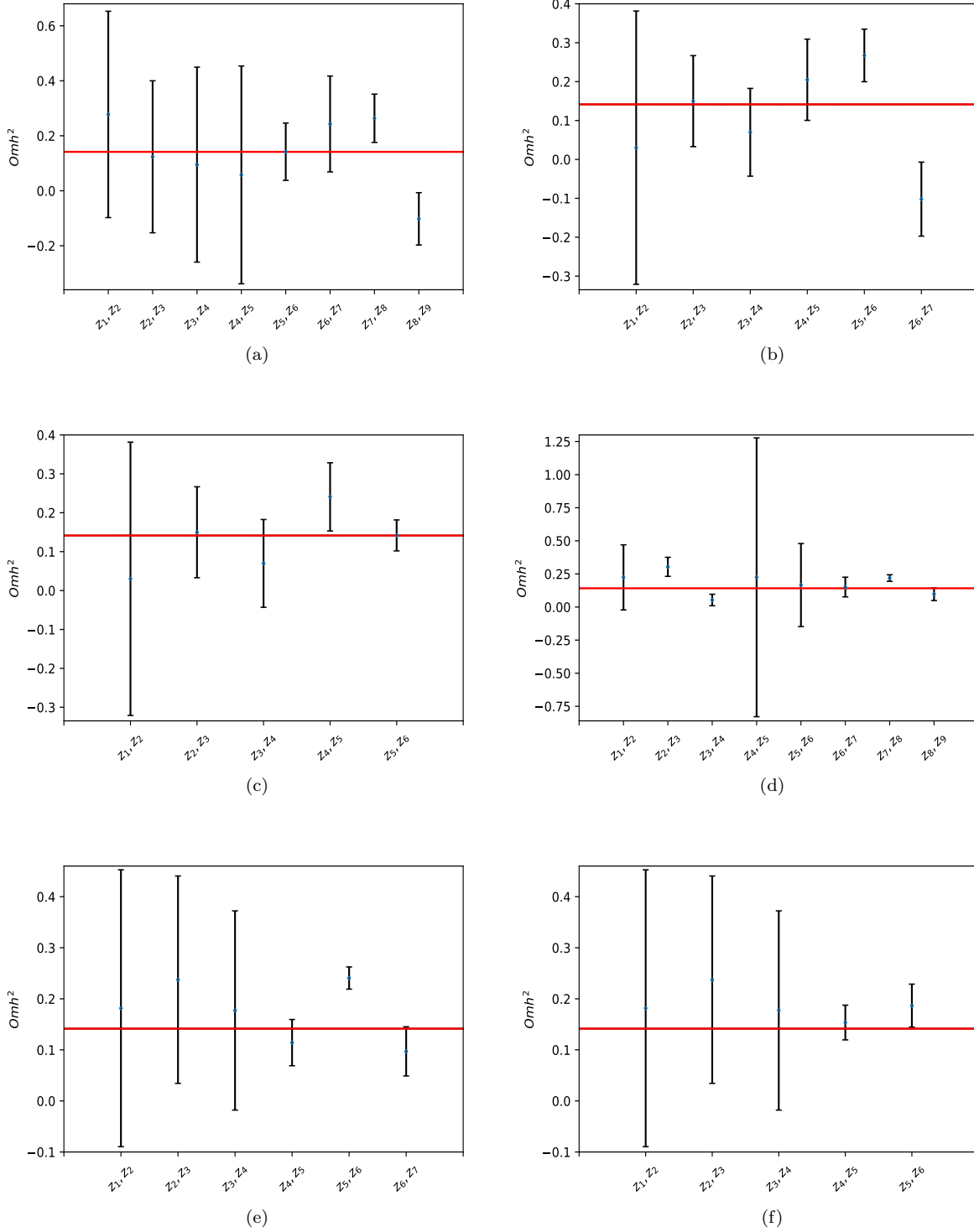


Fig. 7: Same as Fig. 4, but for OHD from the cosmic chronometer method. The panels (a), (b) and (c) present the weighted mean 3-4, 3-4-5, and 5-6 measurements per bin, respectively, and the panels (d), (e) and (f) present the median statistics 3-4, 3-4-5, 5-6 measurements per bin, respectively, where the red lines in the panels represent the best-fit value of $Om h^2$ retrieved from the Planck CMB data.

BAO method are not generally considered to be completely model-independent, even though as mentioned above the fiducial models indeed cannot affect the results (e.g., see Alam et al. [40] P. 5), which means the data are model-independent after all. Nevertheless, due to the trust issue raised by some scientists, we also apply the binning method to the OHD derived from the cosmic chronometer method alone as listed in Tables 4 and 5 for comparison. The results all seem reasonable and, compared to the full binned OHD, the discrepancies are considerably small, which can be the indirect evidence for the validity of the OHD derived from the BAO method. Since the different measurements per bin do not significantly affect the results, we can acknowledge the robustness of the binning methods.

Secondly, combined with the set of binned OHD and, we exploit the $Om h^2(z_2; z_1)$ diagnostic to test if the $Om h^2$ values are constant. From Figs. 2-7, we find that on average the $Om h^2$ values are mostly constant at 1 σ confidence interval. Therefore, the flat Λ CDM model is not invalid. However, this does not mean that the dynamical DE models are not worth considering.

It is worth noticing that more independent OHD would bring more accuracy toward the binning methods, which can result in more reliable $Om h^2(z_2; z_1)$ values. Also, as the number of OHD grows, the binned OHD would be more efficient as a data clarification instrument that can be employed on cosmological constraints. OHD with higher precision and larger amounts are needed and valuable.

Acknowledgements We thank the anonymous referee whose suggestions greatly helped us improve this paper. We thank Remudin Reshid Mekuria for helping us find the typo shown in the figures. This work was supported by National Key R&D Program of China (2017YFA0402600), the National Natural Science Foundation of China (Grants No. 11573006, 11528306), the Fundamental Research Funds for the Central Universities and the Special Program for Applied Research on Super Computation of the NSFC-Guangdong Joint Fund (the second phase).

References

1. J.A. Frieman, M.S. Turner, D. Huterer, Anne. Rev. Astron. Astr. **46**, 385 (2008). DOI 10.1146/annurev.astro.46.060407.145243
2. D.H. Weinberg, M.J. Mortonson, D.J. Eisenstein et al., Phys. Rep. **530**, 87 (2013). DOI 10.1016/j.physrep.2013.05.001
3. A.G. Riess, A.V. Filippenko, P. Challis et al., Astron. J. **116**, 1009 (1998). DOI 10.1086/300499
4. S. Perlmutter, G. Aldering, G. Goldhaber et al., Astrophys. J. **517**, 565 (1999). DOI 10.1086/307221
5. N. Suzuki, D. Rubin, C. Lidman et al., Astrophys. J. **746**, 85 (2012). DOI 10.1088/0004-637X/746/1/85
6. B.A. Benson, T. de Haan, J.P. Dudley et al., Astrophys. J. **763**, 147 (2013). DOI 10.1088/0004-637X/763/2/147
7. S. Dodelson, V.K. Narayanan, M. Tegmark et al., Astrophys. J. **572**, 140 (2002). DOI 10.1086/340225
8. W.L. Freedman, B.F. Madore, V. Scowcroft et al., Astrophys. J. **758**, 24 (2012). DOI 10.1088/0004-637X/758/1/24
9. M. Li, X.D. Li, S. Wang et al., Communications in Theoretical Physics **56**, 525 (2011). DOI 10.1088/0253-6102/56/3/24
10. S. Weinberg, Rev. Mod. Phys. **61**, 1 (1989). DOI 10.1103/RevModPhys.61.1
11. I. Zlatev, L. Wang, P.J. Steinhardt, Phys. Rev. Lett. **82**, 896 (1999). DOI 10.1103/PhysRevLett.82.896
12. G.B. Zhao, M. Raveri, L. Pogosian et al., Nature Astronomy **1**, 627 (2017). DOI 10.1038/s41550-017-0216-z
13. B. Ratra, P.J.E. Peebles, Phys. Rev. D **37**, 3406 (1988). DOI 10.1103/PhysRevD.37.3406
14. C. Wetterich, Nucl. Phys. B **302**, 668 (1988). DOI 10.1016/0550-3213(88)90193-9
15. R.R. Caldwell, Phys. Lett. B **545**, 23 (2002). DOI 10.1016/S0370-2693(02)02589-3
16. C. Armendariz-Picon, V. Mukhanov, P.J. Steinhardt, Phys. Rev. Lett. **85**, 4438 (2000). DOI 10.1103/PhysRevLett.85.4438
17. C. Armendariz-Picon, V. Mukhanov, P.J. Steinhardt, Phys. Rev. D **63**(10), 103510 (2001). DOI 10.1103/PhysRevD.63.103510
18. B. Feng, X. Wang, X. Zhang, Phys. Lett. B **607**, 35 (2005). DOI 10.1016/j.physletb.2004.12.071
19. B. Feng, M. Li, Y.S. Piao et al., Phys. Lett. B **634**, 101 (2006). DOI 10.1016/j.physletb.2006.01.066
20. V. Sahni, A. Shafieloo, A.A. Starobinsky, Phys. Rev. D **78**(10), 103502 (2008). DOI 10.1103/PhysRevD.78.103502
21. C. Zunckel, C. Clarkson, Phys. Rev. Lett. **101**(18), 181301 (2008). DOI 10.1103/PhysRevLett.101.181301
22. A. Shafieloo, V. Sahni, A.A. Starobinsky, Phys. Rev. D **86**(10), 103527 (2012). DOI 10.1103/PhysRevD.86.103527
23. T.J. Zhang, C. Ma, T. Lan, Adv. Astron. **2010**, 184284 (2010). DOI 10.1155/2010/184284
24. L. Yang, H.Y. Wan, T.J. Zhang, T. Yanke, ArXiv e-prints (2017)
25. R. Jimenez, A. Loeb, Astrophys. J. **573**, 37 (2002). DOI 10.1086/340549

26. R. Jimenez, L. Verde, T. Treu et al., *Astrophys. J.* **593**, 622 (2003). DOI 10.1086/376595
27. J. Simon, L. Verde, R. Jimenez, *Phys. Rev. D* **71**(12), 123001 (2005). DOI 10.1103/PhysRevD.71.123001
28. D. Stern, R. Jimenez, L. Verde et al., *J. COSMOL. ASTROPART. P.* **2**, 008 (2010). DOI 10.1088/1475-7516/2010/02/008
29. M. Moresco, A. Cimatti, R. Jimenez et al., *J. COSMOL. ASTROPART. P.* **8**, 006 (2012). DOI 10.1088/1475-7516/2012/08/006
30. C. Zhang, H. Zhang, S. Yuan et al., *Res. Astron. Astrophys.* **14**, 1221 (2014). DOI 10.1088/1674-4527/14/10/002
31. M. Moresco, *Mon. Not. R. Astron. Soc.* **450**, L16 (2015). DOI 10.1093/mnras/slv037
32. M. Moresco, L. Pozzetti, A. Cimatti et al., *JCAP* **5**, 014 (2016). DOI 10.1088/1475-7516/2016/05/014
33. A.L. Ratsimbazafy, S.I. Loubser, S.M. Crawford et al., *Mon. Not. R. Astron. Soc.* **467**, 3239 (2017). DOI 10.1093/mnras/stx301
34. E. Gaztañaga, A. Cabré, L. Hui, *Mon. Not. R. Astron. Soc.* **399**, 1663 (2009). DOI 10.1111/j.1365-2966.2009.15405.x
35. C. Blake, S. Brough, M. Colless et al., *Mon. Not. R. Astron. Soc.* **425**, 405 (2012). DOI 10.1111/j.1365-2966.2012.21473.x
36. L. Samushia, B.A. Reid, M. White et al., *Mon. Not. R. Astron. Soc.* **429**, 1514 (2013). DOI 10.1093/mnras/sts443
37. X. Xu, A.J. Cuesta, N. Padmanabhan et al., *Mon. Not. R. Astron. Soc.* **431**, 2834 (2013). DOI 10.1093/mnras/stt379
38. T. Delubac, J.E. Bautista, N.G. Busca et al., *Astron. Astrophys.* **574**, A59 (2015). DOI 10.1051/0004-6361/201423969
39. A. Font-Ribera, D. Kirkby, N. Busca et al., *J. COSMOL. ASTROPART. P.* **5**, 027 (2014). DOI 10.1088/1475-7516/2014/05/027
40. S. Alam, M. Ata, S. Bailey et al., *Mon. Not. R. Astron. Soc.* **470**, 2617 (2017). DOI 10.1093/mnras/stx721
41. M. Moresco, F. Marulli, *Mon. Not. R. Astron. Soc.* **471**, L82 (2017). DOI 10.1093/mnras/slx112
42. O. Farooq, F. Ranjeet Madiyar, S. Crandall, B. Ratra, *Astrophys. J.* **835**, 26 (2017). DOI 10.3847/1538-4357/835/1/26
43. Planck Collaboration, P.A.R. Ade, N. Aghanim et al., *Astron. Astrophys.* **594**, A13 (2016). DOI 10.1051/0004-6361/201525830
44. L. Samushia, B. Ratra, *Astrophys. J. Lett.* **650**, L5 (2006). DOI 10.1086/508662
45. V. Sahni, A. Starobinsky, *International Journal of Modern Physics D* **9**, 373 (2000). DOI 10.1142/S0218271800000542
46. S.M. Carroll, *Living Rev. Relativ.* **4**, 1 (2001). DOI 10.12942/lrr-2001-1
47. P.J. Peebles, B. Ratra, *Reviews of Modern Physics* **75**, 559 (2003). DOI 10.1103/RevModPhys.75.559
48. E.J. Copeland, M. Sami, S. Tsujikawa, *Int. J. Mod. Phys. D* **15**, 1753 (2006). DOI 10.1142/S021827180600942X
49. T. Clifton, P.G. Ferreira, A. Padilla et al., *Phys. Rep.* **513**, 1 (2012). DOI 10.1016/j.physrep.2012.01.001
50. O. Farooq, S. Crandall, B. Ratra, *Phys. Lett. B* **726**, 72 (2013). DOI 10.1016/j.physletb.2013.08.078
51. S. Podariu, T. Souradeep, J.R. Gott et al., III, *Astrophys. J.* **559**, 9 (2001). DOI 10.1086/322409
52. J.R. Gott, III, M.S. Vogeley, S. Podariu, B. Ratra, *Astrophys. J.* **549**, 1 (2001). DOI 10.1086/319055
53. V. Sahni, A. Shafieloo, A.A. Starobinsky, *Astrophys. J. Lett.* **793**, L40 (2014). DOI 10.1088/2041-8205/793/2/L40

Insert your title here^{*}

Do you have a subtitle?
If so, write it here

First Author^{a,1}, Second Author^{b,2,3}

¹First Address, Street, City, Country

²Second Address, Street, City, Country

³Present Address: Street, City, Country

Received: date / Accepted: date

Abstract Insert your abstract here. Insert your abstract here. Insert your abstract here. Insert your abstract here. Insert your abstract here. Insert your abstract here. Insert your abstract here. Insert your abstract here. Insert your abstract here. Insert your abstract here.

1 Ordinary text

The ends of words and sentences are marked by spaces. It doesn't matter how many spaces you type; one is as good as 100. The end of a line counts as a space.

One or more blank lines denote the end of a paragraph.

Since any number of consecutive spaces are treated like a single one, the formatting of the input file makes no difference to \TeX , but it makes a difference to you. When you use \LaTeX , making your input file as easy to read as possible will be a great help as you write your document and when you change it. This sample file shows how you can add comments to your own input file.

Because printing is different from typewriting, there are a number of things that you have to do differently when preparing an input file than if you were just typing the document directly. Quotation marks like “this” have to be handled specially, as do quotes within quotes: “‘this’ is what I just wrote, not ‘that’”.

Dashes come in three sizes: an intra-word dash, a medium dash for number ranges like 1–2, and a punctuation dash—like this.

A sentence-ending space should be larger than the space between words within a sentence. You sometimes have to type special commands in conjunction with punctuation characters to get this right, as in the following sentence. Gnats,

^{*}Thanks to the title

^ae-mail: magic1@xxx.xx

^be-mail: magic2@xxx.xx

gnus, etc. all begin with G. You should check the spaces after periods when reading your output to make sure you haven't forgotten any special cases. Generating an ellipsis ... with the right spacing around the periods requires a special command.

\TeX interprets some common characters as commands, so you must type special commands to generate them. These characters include the following: & % # { and }.

In printing, text is emphasized by using an *italic* type style.

A long segment of text can also be emphasized in this way. Text within such a segment given additional emphasis with Roman type. Italic type loses its ability to emphasize and become simply distracting when used excessively.

It is sometimes necessary to prevent \TeX from breaking a line where it might otherwise do so. This may be at a space, as between the “Mr.” and “Jones” in “Mr. Jones”, or within a word—especially when the word is a symbol like *itemnum* that makes little sense when hyphenated across lines.

\TeX is good at typesetting mathematical formulas like $x - 3y = 7$ or $a_1 > x^{2n}/y^{2n} > x'$. Remember that a letter like x is a formula when it denotes a mathematical symbol, and should be treated as one.

2 Notes

Footnotes¹ pose no problem.²

3 Displayed text

Text is displayed by indenting it from the left margin. Quotations are commonly displayed. There are short quotations

¹This is an example of a footnote.

²And another one.

This is a short a quotation. It consists of a single paragraph of text. There is no paragraph indentation. and longer ones.

This is a longer quotation. It consists of two paragraphs of text. The beginning of each paragraph is indicated by an extra indentation.

This is the second paragraph of the quotation. It is just as dull as the first paragraph.

Another frequently-displayed structure is a list. The following is an example of an *itemized* list, four levels deep.

- This is the first item of an itemized list. Each item in the list is marked with a “tick”. The document style determines what kind of tick mark is used.
- This is the second item of the list. It contains another list nested inside it. The three inner lists are an *itemized* list.
 - This is the first item of an enumerated list that is nested within the itemized list.
 - This is the second item of the inner list. \LaTeX allows you to nest lists deeper than you really should.

This is the rest of the second item of the outer list. It is no more interesting than any other part of the item.
- This is the third item of the list.

The following is an example of an *enumerated* list, four levels deep.

1. This is the first item of an enumerated list. Each item in the list is marked with a “tick”. The document style determines what kind of tick mark is used.
2. This is the second item of the list. It contains another list nested inside it. The three inner lists are an *enumerated* list.
 - (a) This is the first item of an enumerated list that is nested within the enumerated list.
 - (b) This is the second item of the inner list. \LaTeX allows you to nest lists deeper than you really should.

This is the rest of the second item of the outer list. It is no more interesting than any other part of the item.
3. This is the third item of the list.

The following is an example of a *description* list.

Cow Highly intelligent animal that can produce milk out of grass.

Horse Less intelligent animal renowned for its legs.

Human being Not so intelligent animal that thinks that it can think.

You can even display poetry.

There is an environment for verse
Whose features some poets will curse.
For instead of making
Them do *all* line breaking,
It allows them to put too many words on a line when
they’d rather be forced to be terse.

Mathematical formulas may also be displayed. A displayed formula is one-line long; multiline formulas require special formatting instructions.

$$x' + y^2 = z_i^2$$

Don’t start a paragraph with a displayed equation, nor make one a paragraph by itself.

Example of a theorem:

Lemma 1 *All conjectures are interesting, but some conjectures are more interesting than others.*

Proof Obvious. □

4 Tables and figures

Cross reference to labelled table: As you can see in Table 1 on page 3 and also in Table 2 on page 3.

A major point of difference lies in the value of the specific production rate π for large values of the specific growth rate μ . Already in the early publications [1–3] it appeared that high glucose concentrations in the production phase are well correlated with a low penicillin yield (the ‘glucose effect’). It has been confirmed recently [1–4] that high glucose concentrations inhibit the synthesis of the enzymes of the penicillin pathway, but not the actual penicillin biosynthesis. In other words, glucose represses (and not inhibits) the penicillin biosynthesis.

These findings do not contradict the results of [1] and of [4] which were obtained for continuous culture fermentations. Because for high values of the specific growth rate μ it is most likely (as shall be discussed below) that maintenance metabolism occurs, it can be shown that in steady state continuous culture conditions, and with μ described by a Monod kinetics

$$C_s = K_M \frac{\mu/\mu_x}{1 - \mu/\mu_x} \quad (1)$$

Pirt and Rhigelato determined π for μ between 0.023 and 0.086 h⁻¹. They also reported a value $\mu_x \approx 0.095$ h⁻¹, so that for their experiments μ/μ_x is in the range of 0.24 to 0.9. Substituting K_M in (1) by the value $K_M = 1$ g/L as used by [1], one finds with the above equation $0.3 < C_s < 9$ g/L. This agrees well with the work of [4], who reported that penicillin biosynthesis repression only occurs at glucose concentrations from $C_s = 10$ g/L on. The conclusion is that the glucose concentrations in the experiments of Pirt and Rhigelato probably were too low for glucose repression to be detected. The experimental data published by Ryu and Hospodka are not detailed sufficiently to permit a similar analysis.

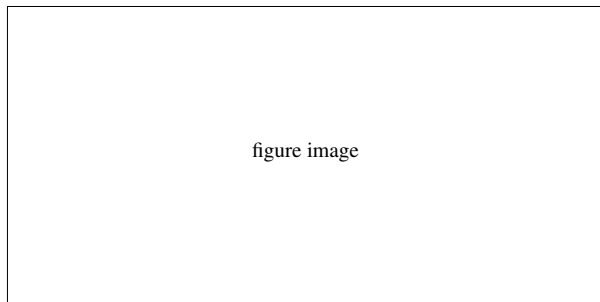
Bajpai and Reuß decided to disregard the differences between time constants for the two regulation mechanisms (glucose repression or inhibition) because of the relatively

Table 1 The spherical case ($I_1 = 0, I_2 = 0$)

Equil. Points	x	y	z	C	S
L_1	-2.485252241	0.000000000	0.017100631	8.230711648	U
L_2	0.000000000	0.000000000	3.068883732	0.000000000	S
L_3	0.009869059	0.000000000	4.756386544	-0.000057922	U
L_4	0.210589855	0.000000000	-0.007021459	9.440510897	U
L_5	0.455926604	0.000000000	-0.212446624	7.586126667	U
L_6	0.667031314	0.000000000	0.529879957	3.497660052	U
L_7	2.164386674	0.000000000	-0.169308438	6.866562449	U
L_8	0.560414471	0.421735658	-0.093667445	9.241525367	U
L_9	0.560414471	-0.421735658	-0.093667445	9.241525367	U
L_{10}	1.472523232	1.393484549	-0.083801333	6.733436505	U
L_{11}	1.472523232	-1.393484549	-0.083801333	6.733436505	U

Table 2 Parameter sets used by Bajpai and Reuß

parameter		Set 1	Set 2
μ_x	[h ⁻¹]	0.092	0.11
K_x	[g/g DM]	0.15	0.006
μ_p	[g/g DM h]	0.005	0.004
K_p	[g/L]	0.0002	0.0001
K_i	[g/L]	0.1	0.1
$Y_{x/s}$	[g DM/g]	0.45	0.47
$Y_{p/s}$	[g/g]	0.9	1.2
k_h	[h ⁻¹]	0.04	0.01
m_s	[g/g DM h]	0.014	0.029

**Fig. 1** Pathway of the penicillin G biosynthesis

very long fermentation times, and therefore proposed a Haldane expression for π .

It is interesting that simulations with the [4] model for the initial conditions given by these authors indicate that, when the remaining substrate is fed at a constant rate, a considerable and unrealistic amount of penicillin is produced when the glucose concentration is still very high [2-4] Simulations with the Bajpai and Reuß model correctly predict almost no penicillin production in similar conditions.

Sample of cross-reference to figure. Figure 1 shows that is not easy to get something on paper.

5 Headings

5.1 Subsection

Carr-Goldstein based their model on balancing methods and biochemical knowledge. The original model (1980) contained an equation for the oxygen dynamics which has been omitted in a second paper (1981). This simplified model shall be discussed here.

5.1.1 Subsubsection

Carr-Goldstein based their model on balancing methods and biochemical knowledge. The original model (1980) contained an equation for the oxygen dynamics which has been omitted in a second paper (1981). This simplified model shall be discussed here.

6 Equations and the like

Two equations:

$$C_s = K_M \frac{\mu/\mu_x}{1 - \mu/\mu_x} \quad (2)$$

and

$$G = \frac{P_{\text{opt}} - P_{\text{ref}}}{P_{\text{ref}}} 100 (\%) \quad (3)$$

Two equation arrays:

$$\frac{dS}{dt} = -\sigma X + s_F F \quad (4)$$

$$\frac{dX}{dt} = \mu X \quad (5)$$

$$\frac{dP}{dt} = \pi X - k_h P \quad (6)$$

$$\frac{dV}{dt} = F \quad (7)$$

and,

$$\mu_{\text{substr}} = \mu_x \frac{C_s}{K_x C_x + C_s} \quad (8)$$

$$\mu = \mu_{\text{substr}} - Y_{x/s}(1 - H(C_s))(m_s + \pi/Y_{p/s}) \quad (9)$$

$$\sigma = \mu_{\text{substr}}/Y_{x/s} + H(C_s)(m_s + \pi/Y_{p/s}) \quad (10)$$

Acknowledgements If you'd like to thank anyone, place your comments here and remove the percent signs.

Appendix A: Appendix section

We consider a sequence of queueing systems indexed by n . It is assumed that each system is composed of J stations, indexed by 1 through J , and K customer classes, indexed by 1 through K . Each customer class has a fixed route through the network of stations. Customers in class k , $k = 1, \dots, K$, arrive to the system according to a renewal process, independently of the arrivals of the other customer classes. These customers move through the network, never visiting a station more than once, until they eventually exit the system.

Appendix subsection

However, different customer classes may visit stations in different orders; the system is not necessarily "feed-forward." We define the *path of class k customers* in as the sequence of servers they encounter along their way through the network and denote it by

$$\mathcal{P} = (j_{k,1}, j_{k,2}, \dots, j_{k,m(k)}). \quad (\text{A.1})$$

Sample of cross-reference to the formula (A.1) in [Appendix A](#).

Appendix B: Appendix section

We consider a sequence of queueing systems indexed by n . It is assumed that each system is composed of J stations, indexed by 1 through J , and K customer classes, indexed by 1 through K . Each customer class has a fixed route through the network of stations. Customers in class k , $k = 1, \dots, K$, arrive to the system according to a renewal process, independently of the arrivals of the other customer classes. These customers move through the network, never visiting a station more than once, until they eventually exit the system.

References

1. S. Chekanov et al. (ZEUS Collaboration), *Eur. Phys. J. C* **42**, 1 (2005)
2. P.C. Brans, U.G. Meissner, *Eur. Phys. J. C* **40**, 97 (2005)
3. N. Kersting, *Eur. Phys. J. C* (2009). doi:10.1140/epjc/s10052-009-1063-6
4. J.M. Smith, *Molecular Dynamics*, 2nd edn. (Springer, Berlin, Heidelberg, 1987)
5. J.M. Smith, in *Molecular Dynamics*, ed. by C. Brown, 2nd edn. (Les Editions de Physique, Les Ulis, 1987)
6. J.M. Smith, in *Molecular Dynamics*, ed. by C. Brown, 2nd edn. (Springer, Berlin, Heidelberg, 2009 in press)
7. J.M. Smith, in *Proceedings of the International Conference on Low Temperature Physics, Madison, 1975*, ed. by C. Brown (Les Éditions de Physique, Les Ulis, 1975), p. 201
8. J. Cartwright, Big stars have weather too. (IOP Publishing PhysicsWeb, 2007), <http://physicsweb.org/articles/news/11/6/16/1>. Accessed 26 June 2007